Genesis and Uniformity of Some Soils in West El-Minia, Western Desert, Egypt

Adel A. Elwan

Pedology Department, Water Resources and Desert Soils Division, Desert Research Center (DRC), Cairo, 11753, Egypt

*Corresponding author: E-mail: dr.elwandrc@gmail.com

DOI: 10.21608/JALEXU.2022.113069.1032

Article Information

Received:November 25th 2021

Revised: December 27th 2021

Accepted:December 29th 2021

Published: December 31st 2021

ABSTRACT: A total of 216 pedons were regularly distributed throughout 130,000 Faddan across the Darb Al-Bahnsawy area at West El-Minia Governorate, Central Egypt representing the major variations in the site. Soil pedons were pedomorphologically described and soil samples were collected from genetic horizons. The toposequence soil transect across a slope gradient (95-135 m) was selected for identifying the origin and homogeneity of the soils under study. To demonstrate uniformity or discontinuity of parent material, the weathering indices of Wr1, Wr2, and Wr3 were performed besides uniformity indices of UV1 and UV2. Five different soil types were distinguished based on soil depth, soil texture, and surface topography. The investigated soils were coarse-textured and widely varied from deep (>100cm) to shallow (<50 cm). Moreover, they also were classified into different categories based on the gypsum content; slightly gypsiric, moderately gypsiric, and strongly to extremely gypsiric soils, and the *gypsic* horizons were developed on upper slopes. Some studied soils were affected by the calcareous nature. The investigated soils had different horizonation sequences which are C-2Cyy for shallow soil, C1-C2-2Cyy and C-2C1yy-2C2yy for moderately deep soils, C-Ck-2Cy-2Cr and C-Ck-2C-3C for deep soils. Most soils were formed through geologic processes with no evidence of pedogenesis, except for *calcic* horizons (Ck) formed on lower slope soils, and *gypsic* horizons (2C1yy and 2C2yy) formed on upslope soils over the studied toposequence transect. Lithologic discontinuities in most pedons revealed sequences of deposition and erosion processes and the heterogeneity of the parent material. The difference in sand and silt separates of UV1 index on a carbonate-free and clay-free basis was consistent with the vertical distribution of rock fragments within the pedon. The light minerals associations in the studied soils were dominated by quartz, gypsum, feldspars, calcite, mica, and chlorite. Heavy mineral percentages (1.46 – 16.34%) were increased from the west to the east of the investigated transect across the slope gradient. The highest concentration of heavy minerals (10.09 – 16.34%) was detected in the lower soils. The identified heavy minerals were pyroxene (augite and hyperthene), amphiboles (hornblende and actinolite), garnet, staurolite, kyanite, zircon, tourmaline, rutile, epidote, zoisite, biotite, monazite, glaconite, and opaques. Opaque minerals (39.33 to 61.33%) constitute the most predominant constituent in all studied soil samples. The heavy minerals characteristics suggest their mixed sources from sandstone, limestone, and metamorphic rocks. Limestone plateau was the main source of soil regolith, the uniformity ratios depict heterogeneous distribution with depth that may be due to the sedimentation processes which act upon most soils. The sediments were immature to submature based on ZTR index. Various genetic stages of *gypsic* horizons development were proposed in the current study. Gypsum materials originated within the studied sediments from the weathering of the surrounding Eocene white limestone plateau. The results of weathering indices curves demonstrated that the soils under study are formed from multi-origin under multi-depositional regimes.

Keywords: Pedon, genesis, *gypsic* horizon, *calcic* horizon, uniformity, West El-Minia, Central Egypt.

INTRODUCTION

Pedology is a scientific and applied field for identifying the soil-forming processes and factors in the semi-arid and arid zones around the world **(**Madakka et al., 2021**).** Soils across a slope gradient will be developed and evolved in an interdependent manner under the same parent material (Bockheim et al., 2005; Baillie et al., 2021). A catena is a set of a series of similar soils on a slope under a given topographic situation and climatic criteria. Soil slope is a dynamic contributor to occur the pedogenic processes and

varies the types of soils across diverse landforms and landscapes (Kapur et al., 2018; Madakka et al., 2021). In dryland, soil parent materials can discriminate main types of soils which are primarily related to pedogenic processes such as accumulation of gypsum, carbonates, and soluble salt vertically within the pedon horizons. Soil development occurs on the land surface in which the soils may be formed on different catenas. Regolith or soil formation may be occurred based on the balance between inputs and losses of soil materials at different geological timescales. To form parent material, the loose sediments of inorganic material or weathered inputs from in-situ rocks may be translocated via water or air carrying the soluble salts and atmospheric dust and deposited at specific slope positions (Soares et al., 2020). Dissolved losses and solutes such as gypsum and carbonates are transported from the surficial weathering zone and the net mass of additional dust and solutes accumulated in the horizons of soil pedons due to the chemical weathering (Baillie et al., 2021). In arid regions, the long-term soil development process is occurred slowly due to the scarcity of rainfall which is required for chemical weathering and leaching, and therefore the dissolved losses are reduced (Elwan, 2018). Gypsum constituent is a sulfate mineral in soils of semi-arid to arid regions around the world. Its contents widely vary between less than 2% and more than 90% based on the parent material origin, slope, and climate of the area (Lizzoli et al., 2021). Soil moisture regime is the most contributor to the occurrence and accumulation of gypsum materials in the soils than the soil temperature regime (Salman et al., 2021). Gypsum crystals may be occurred as individuals or as masses within the soil pedon horizons. Furthermore, they can soft materials or cemented horizons (Lizzoli et al., 2021).

Soil parent material archive may be utilized as a powerful indicator for investigating climate changes across different lands of desert ecosystems. The variations in soil properties across landscape positions are usually attributed to the changes in climate, soil runoff, erosion, and sedimentation processes which affect soil origin and uniformity (Sulieman et al., 2021). Numerous studies of drylands in arid regions of desert ecosystems show that soils are varied in topography, water distribution, parent material, age of the land surface, amount and intensity of rainfall, and plant heterogeneity (Baillie et al., 2021). The study of parent material uniformity is a very vital and suitable media for assessing pedological processes and forming the soils **(**Lizzoli et al., 2021). The immobile and resistant minerals to chemical weathering in arid soils were a powerful basis to assess alterations of horizons vertically within soil pedons and indicate the soil genesis rocks (Moghbeli et al., 2021). The resistant heavy minerals and their distributions vertically within the upper horizons of solum have been utilized to distinguish between pedological and geological processes (**Siqueira** et al., 2021). Varied species of heavy minerals have been employed but the most common minerals in dry soils are quartz, xenotime, zircon, tourmaline, and rutile (Salman et al., 2021).

Sediment provenance can be measured by sensitive indicators of heavy mineral assemblages. Many species of the heavy mineral are found in sandstone and limestone which have restricted paragenesis. These resistant minerals can indicate the composition of minerals and source rocks. Variances in heavy mineral assemblages vertically across soil pedon layers facilitate the identification of soil origin derived from different sources and pedon uniformity via different sediment transport pathways.

Limestone is considered as carbonate rocks that represent about 10 percent of land surface and occupy 20 percent of the sedimentary rocks around the world (Pinheiro Junior et al., 2021) and therefore represent a major soil parent material, particularly in Egypt. Furthermore, gypsum rocks are also considered a major component of the sedimentary rocks, and therefore a wide extent of lithology was found in Egypt (Elwan, 2018). Accordingly, pedological knowledge and soil investigations should be implemented to understand the impact of this lithology on soil genesis and pedon uniformity. In this accord, the main aims of the current research paper were to (1) map the major types of studied soils; (2) characterize the pedological processes affecting the soil formation and evolution; and (3) assess the genesis, maturity, and uniformity of the soil parent material.

MATERIALS AND METHODS

Study site Description

The study was conducted in the Darb Al-Bahnsawy area, West El-Minia, in the Western Desert, Central Egypt. The study area is located west of the River Nile and bounded by the western limestone plateau within the boundary of El-Minia Governorate (Fig. 1). It lies between longitudes of 29°35′ & 30°01′E and latitudes of 28°07′ & 28°25′N (Fig. 1). It covers an area of about 135000 Faddan. Many asphaltic roads and desert loggers are available to access the study area. The arid climate with hot summer, warm winter, high evaporation, and low rainfall intensity are the main characteristics of the study area. The meteorological criteria of the El-Minia station were recorded for 30 years (1990–2020). The minimum air temperature ranges from 5°C to 21°C in January and August, respectively. Whereas, the maximum temperature varies between 25.5 °C and

43.5°C in January and June, respectively. Rainfall is usually rare throughout the region where the rainy months starting from October to the end of May; the annual precipitation rate is 19.6 mm/year. The maximum rainfall in one day of rain and heavy storms is 7.6 mm/day in October. Therefore, the contribution of rainfall to groundwater recharge is expected to be scarce. Recently, climate change patterns could occur in random ways. In the present study, four geomorphologic units were identified including; the tableland, isolated hills, three flood plains (silt plain, sandy plain, and gravely plain) (Shabana, 2010), and sand dunes belt of the Western Desert which started from the south Qattara Depression and extended to the West El-Minia **(**Salem, 2015; Yousif et al., 2018).

The Eocene white limestone is exposed on both east and west sides of the River Nile within the boundary of El-Minia Governorate, Central Egypt. This led to forming vertical scarps above the flood plain of River Nile and therefore persistent plateaus were developed in the east and west of the valley. These scarps and plateaus are made up of the El-Minia formation at the base and the Samalut formation at the top as shown in Fig. (2) (Lotfy et al., 2017). El-Minia and Samalut formations belong to the Eocene rocks in the investigated area. Samalut formation is composed of chalky limestone with thin silt and clay intercalations. Geology knowledge has a key role in the quality and occurrence of groundwater in the study area. Consequently, the lithostratigraphy of the water-bearing formations and hydrogeological structure needs to be evaluated adequately (El-Rawy et al., 2021). There are six major aquifers across different locations in Egypt these aquifers are the Nubian Sandstone aquifer, Nile aquifer, Al-Moghra aquifer, Fissured Carbonate aquifer, Fissured Hard-rock aquifer, and Coastal aquifer (Abu-Bakr, 2020). East El-Minai is mainly supported by the Nile aquifer which belongs to the Quaternary age. This aquifer is highly productive and is composed of gravel and sand. Its thickness reached 400 m (Abu-Bakr, 2020).

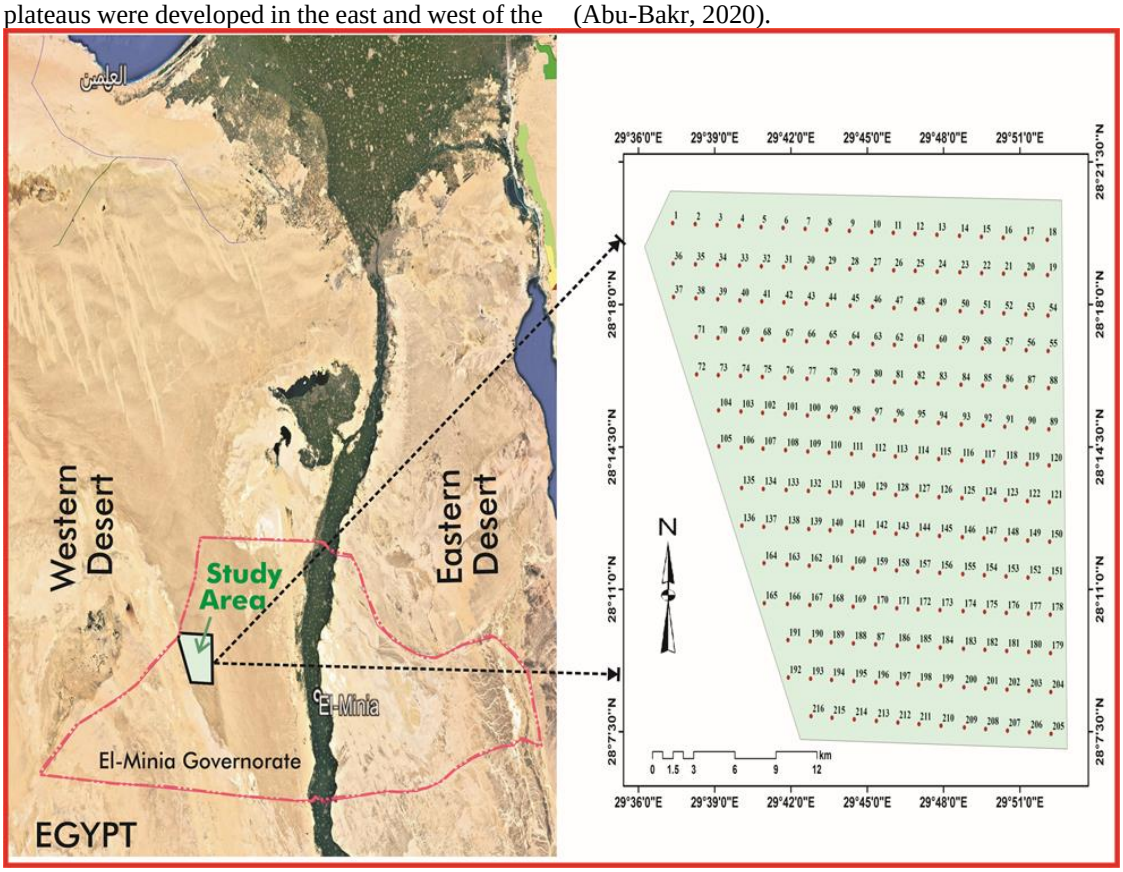

Fig.1. Location map of the study area within the El-Minia Governorate boundary showing a regular grid of pedon locations across the study area.

Numerous lithologic units were exposed across the lands of the study area in age from the Middle Eocene to the Quaternary (Yousif et al., 2018) (Fig. 2). These units include, from top to base, Quaternary alluvial deposits, Katkut Formation, Qatrani Formation, Samalut Formation, and El-Minia Formation (El-Rawy et al., 2021). Formations of El-Minia and Samalut belong to Eocene time and are composed mainly of weathered carbonate rocks in the study area (Lotfy et al., 2017). The age of exposed rocks in the study area varies from Lower Eocene to Quaternary. Eocene and Oligocene rocks are covering most land on the surface of the study area. The sediments of Nile silt, sand dunes, Prenile, and proto-nil belong to the recent Quaternary. The study area is

affected by a network of faulting systems. These faults play a great role in the occurrences of the groundwater aquifers in West El-Minia (Yousif et al., 2018). One water-bearing formation was identified in the West El-Minia area including the Middle Eocene limestone aquifer (Shabana, 2010). The Nubian and Oligocene sandstones were recorded as water-bearing formations in the study area (Yousif et al., 2018) (Fig. 2). The water of the River Nile is insufficient for achieving water security in Egypt. This is due to climate change, population growth, water contamination, irregular distribution of water resources, and development projects in the Nile River basin (Yousif et al., 2018).

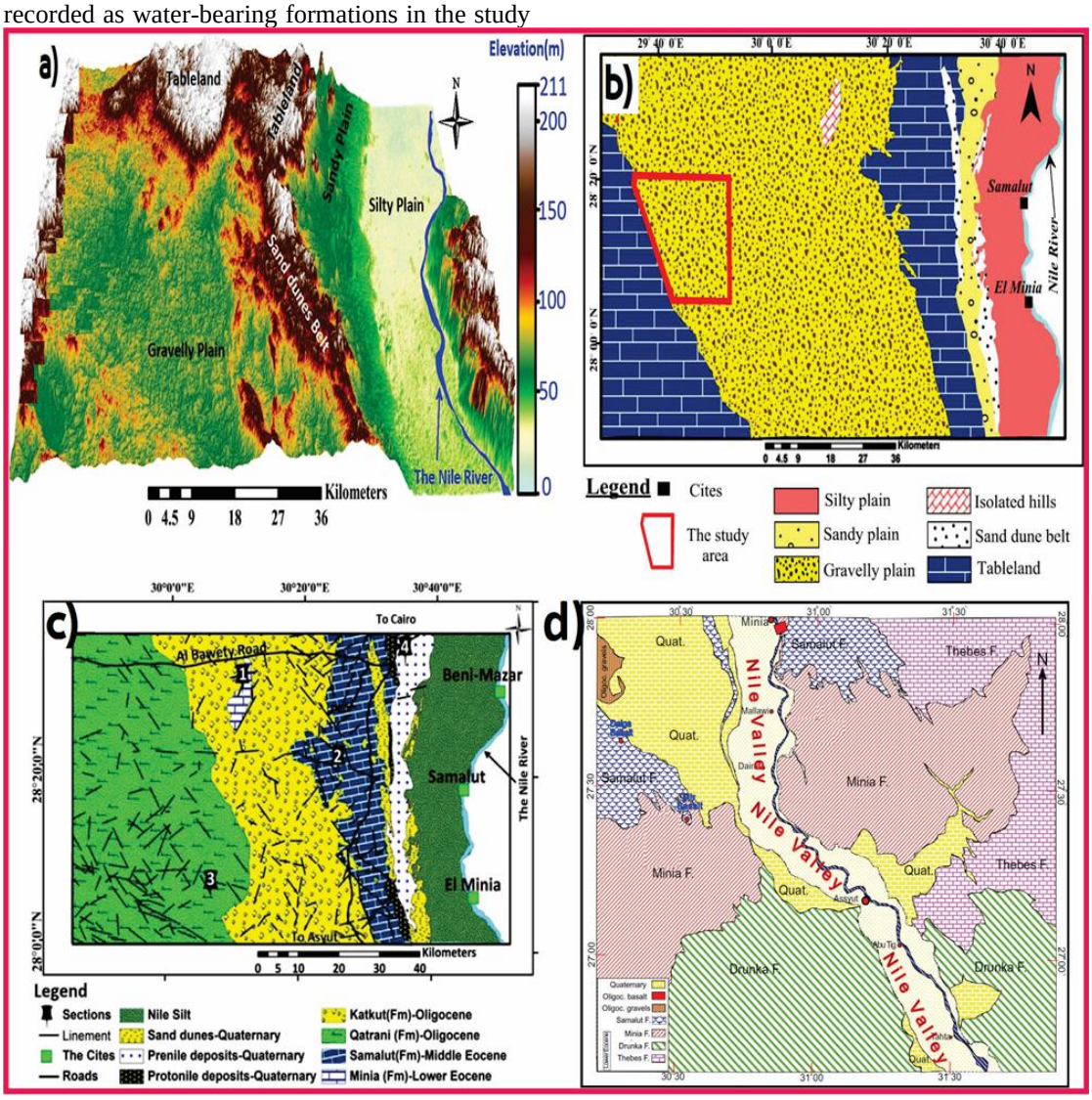

Fig. 2. Geomorphological and geological setting of the study area; a) Three-dimensional view showing the main landforms of the West El-Minia region, B), b) Geomorphology map of the study area, and c) Geology map of the study area, and d) Geological formations (modified after Lotfy et al., 2017; Yousif et al., 2018).

Fieldwork

A total of 216 pedons were regularly distributed throughout 130,000 Faddan across the study area in West El-Minia representing the major variations in the site (Fig. 1). Pedons from a soil transect across a soil toposequence were collected from West El-Minia, Egypt (Figs. 2 and 3). Using manuals of Schoeneberger et al. (2012) and Soil Science Division Staff (2017), pedons were described and soil samples were taken from genetic horizons. For distinction, definition, and designation of genetic horizons, Soil Survey Staff (2014a) and FAO (2006) were considered. The morphological and physicochemical characters were used to identify the soil types and classify them into soil mapping units. Based on the hypothesis that topography might be the main controlling factor in soil development, soils of the study area have been studied along a representative topographical transect within the study area from the west at the plateau to the east across the gravelly alluvial plain (Figs. 2 and 3). The top

sequence transect ran horizontally across a slope gradient in the alluvial plain landscape from the west at a higher slope (125-150 m above sea level) to the east at the lower slope (95-120 m above sea level) (Fig. 3). Soils were sampled by genetic horizon from gravelly plain across environmental gradients. Detailed morphological descriptions of each horizon/layer of representative pedons and their sites were made in the field itself as per the standards procedures given by FAO (2006), Schoeneberger et al. (2012), and Soil Science Division Staff (2017). Soil color was determined for moist samples using the Munsell notation (Munsell Color, 2009).

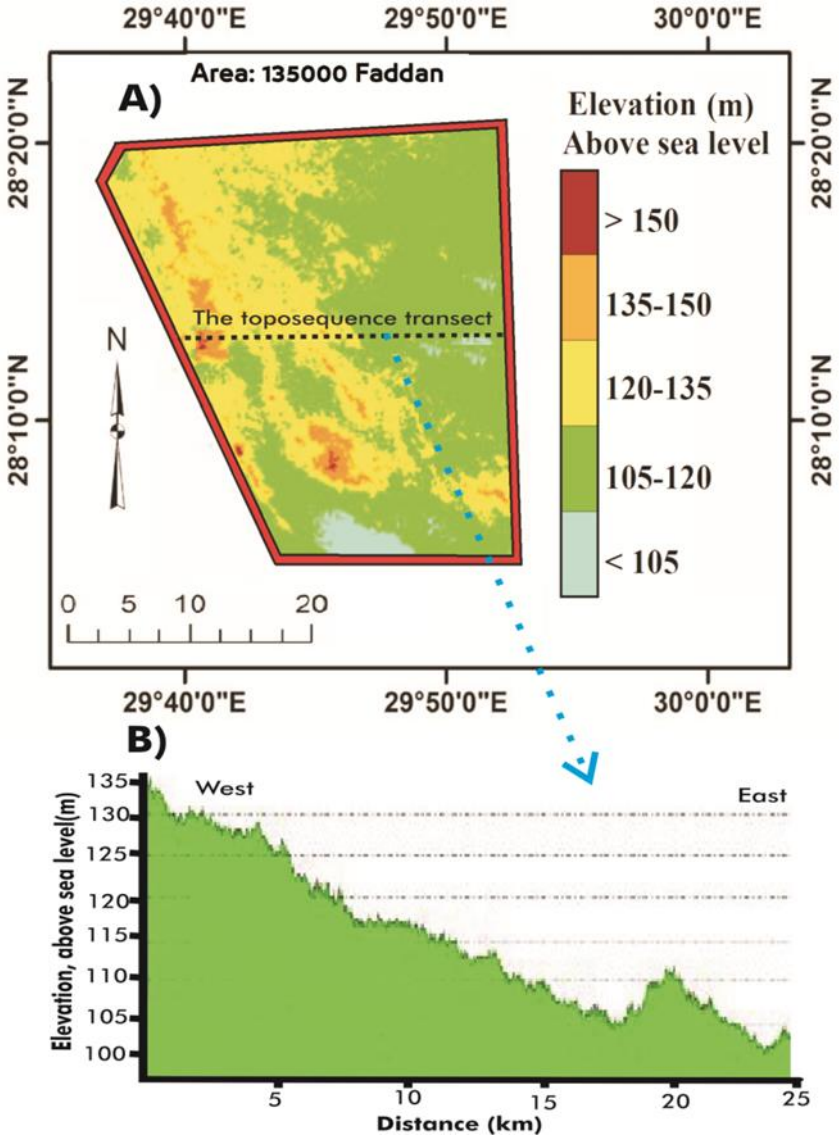

Fig. 3. Ground elevations above sea level; A) Digital elevation model for the study area, B) the Toposequence transect (Topographical profile) across the gravelly alluvial plain from the west to the east.

A wider range of classification terminology was used by different international sources to identify the soils derived from gypsum-rich parent material based on the gypsum content of a soil's fine earth fraction. The world reference base for soil resources (IUSS Working Group WRB, 2015) uses gypseous soils under two names; the first is *hypogypsic* (<25% gypsum, $CaSO_4.2H_2O$) and the second is *hypergypsic* (>50% gypsum) as qualifiers. The *gypsiferous* soil term was used by Soil Science Division Staff (2017) for the material that contains 15 to less than 40 percent, by weight, gypsum. While the fine gypsum material term or coarse gypsum material was used for material that has 40 percent or more gypsum (Soil Science Division Staff, 2017). Furthermore, FAO (2006) designates gypsiric terms for the soil affected by gypsum under different categories (non-gypsiric, slightly gypsiric, moderately gypsiric, strongly gypsiric, and extremely gypsiric).

Analyses work

Soil samples were air-dried and hand-sieved through a 2-mm screen to remove roots, stone, and other debris. The sand fractions were determined by dry sieving following the Wentworth classes (Soil Science Division Staff, 2017). The silt and clay fractions were determined using the pipette method after removing organic matter digesting it in a heated hydrogen peroxide solution and using sodium hexametaphosphate as the dispersing agent (Su et al., 2004). Some soil physicochemical analyses were carried out according to the methods described by the Pansu and Gautheyrou (2006) and Soil Survey Staff (2014b). Sample weight and volume were corrected for coarse fragment content (Soil Survey Staff, 2014b). Gypsum concentration was determined by the differential water loss method (Artieda et al., 2006).

Uniformity and maturity indices

The detection of lithologic discontinuities (LDs) was based on the nonuniformity of the parent material (Schaetzl and Anderson, 2005). Field and laboratory data sets were evaluated in-depth function as a visual estimation of rock fragments which is used in this paper to detect the LDs. The difference in the grain size of soil (silt and sand) was studied using the uniformity value index (UV1) (Cremeens and Mokma, 1986) (Formula 1). The UV1 index compares particle size data from the horizon/layer above.

$$\mathbf{UV1} = \frac{[(\mathbf{Si} + \mathbf{VFS})/(\mathbf{S} - \mathbf{VFS})]\ \mathbf{in\ overlaying\ horizon/layer}}{[(\mathbf{Si} + \mathbf{VFS})/(\mathbf{S} - \mathbf{VFS})]\ \mathbf{in\ overlaying\ horizon/layer}} - \mathbf{1} \qquad (\mathbf{1})$$

Where UV1 is a uniformity value index of Cremeens and Mokma (1986). Si is silt content, VFS is very fine sand content, and S stands for whole sand content.

Another method was suggested by Kowalska et al. (2016) for the calculation of uniformity values (UV2) that considers the whole granulometric fraction in the soil (clay, silt, and sand) (Formula 2). In the current study, this method is applied and tested against the UV1 method.

$$\mathbf{UV2} = \frac{[(\mathbf{C} + \mathbf{Si})/(\mathbf{S})]\ \mathbf{in\ overlaying\ horizon/layer}}{[(\mathbf{C} + \mathbf{Si})/(\mathbf{S})]\ \mathbf{in\ overlaying\ horizon/layer}} - \mathbf{1} \qquad (\mathbf{2})$$

Where UV2 is the uniformity value index of Kowalska et al. (2016), *C* is clay content, *Si* is silt content, and *S* stands for sand content.

The closer the UV1 or UV2 is to zero, the more likely that the two horizons or layers in a pedon formed from similar parent materials. Values higher than 0.60 indicate the presence of a lithologic discontinuity (LD) and nonuniformity of the parent material (Cremeens and Mokma, 1986; Schaetzl and Anderson, 2005).

Interpretation of the distribution of the heavy mineral has been carried out to detect the uniformity of soil parent material. The concept is based on the fact that heavy minerals residue has a wide range of mineral species. The index minerals are considered more resistant to processes of soil formation than the other species. The ratios (Wr1, Wr2, and Wr3) among the non-resistance and resistance minerals were used as criteria for investigating parent material uniformity across a pedon; and consequently soil development (Equations 3, 4, and 5).

Wr1= (Pyroxene + Amph) / (Zir + Tourmaline)	(**3**)
Wr2=Horn /(Zir + Tourmaline),	(**4**)
Wr3 = Biotite /(Zir + Tourmaline).	(**5**)

Moreover, the ZTR maturity index is the percentage of the combined zircon, tourmaline, and rutile among the total non-opaque heavy minerals (Equation 6). The three minerals have high mechanical and chemical stability to wear and tear. Less resistant unstable minerals are dissolved when the maturity of the sediments increases. Most resistant minerals remain almost unchanged and their relative abundance to their counterparts in sediment increases. This is the reason why the percentage of these resistant minerals can express the sediment's maturity.

$$\mathbf{ZTR = [(\ zircon + tourmaline + rutile)/(\Sigma\ non\text{-}opaques)] \times 100} \qquad \mathbf{(6)}$$

Microscopic methods

To determine the mineral composition of heavy and light mineral associations, all samples were sieved to the 63-250 μm size fraction. This fraction was selected for the analysis because it includes all virtual mineral species in proportions representative of the bulk sample. The standard procedures of Mange and Maurer (1992) and Mange and Wright (2007) were applied to separate and prepare the heavy minerals in the concerned samples from studied pedons. Each sediment sample was first treated with 30% hydrogen peroxide to remove the organic matter. It was then decalcified with 20% hydrochloric acid. The heavy minerals were separated from this fraction using bromoform ($CHBr_3$) at a density of 2.85-2.88 g cm^{-3}. The heavy minerals were mounted on glass slides and identified using a petrographic (polarizing) microscope with the counting results expressed as percentages. Canada balsam was used as the mounting medium. The abundance of each non-opaque mineral was calculated as a percentage of the total grains counted for each sample.

RESULTS AND DISCUSSION

Soil Morphological and Physicochemical Characteristics

Field morphological attributes, physicochemical data, and uniformity indices for the five typical pedons are presented in Table (1). All pedons under investigation are vertically differentiated for different layer sequences in terms of their morphology and texture (Fig. 4). Five different soil types were distinguished based on soil depth, soil texture, and surface topography as shown in Fig. (3). The area covered an area of about 130,000 thousand Faddan. They were identified across the study area. The soil mapping units (SMUs) are (i) deep, coarse-textured soils with almost flat to gently undulating topography surface, (ii) deep, coarse-textured soils with gently undulating to undulating topography, (iii) moderately deep, coarse-textured soils with almost flat topography, (iv) moderately deep, coarse-textured soils with undulating topography, and (v) shallow, coarse-textured soils with almost flat to undulating topography. The first soil mapping unit (SMU1) was developed on the lower slopes position. It occurred on nearly level slopes dominated by deep (> 100 cm) coarse-textured soils (sands, loamy sand, loamy coarse sand) (Table 1; Fig. 4).

Most layers of the studied pedons have loose to very friable consistence, whereas the lower horizons of SMU1 and SMU2 were firm or very firm in moist consistency. The evidence of reduced soil matrices was found within the pedons of SMU1 and SMU2 and their horizons exhibited common, faint, finely disseminated iron depletion. Redox concentrations in the lower horizons of these pedons appeared in the form of oxidized iron (Fe^{+3}) masses in the matrix around depletions. By contrast, the carbonate effervescence was low in *gypsic* horizons (Cy, Cyy) and higher in *calcic* horizons (Ck) as finely disseminated carbonates or masses indicative of their origin from the upper limestone plateau. In general, soils in the study area have a structureless (single grain and massive) where the soil is a regolith. Some regolith layers present massive to single grain as structureless, which are neither plastic nor sticky. Crust-related and trans-horizon were identified in the upper horizons in soils of SMU1, SMU2, and SMU3. Crust-related cracks were formed as shallow at the regolith surface as seen in pedons of SMU1 (Fig. 6). Trans-horizon cracks were found in the pedons of SMU2 and extended from the regolith surface to 80 cm depth as shown in the C, Ck, and 2Cy horizons. Gypsum is accumulated as crystal clusters, non-cemented to slightly cemented masses, and finely disseminated gypsum in the horizons of Cy and Cyy occurred in SMU3, SMU4, and SMU5. Gypsum was rarely found cemented across studied pedons. Soils of the study area were classified into three categories based on the gypsum content. Slightly gypsiric soils (<5% $CaSO_4.2H_2O$), moderately gypsiric soils (5-15% $CaSO_4.2H_2O$), and strongly to extremely (>15 to >60% $CaSO_4.2H_2O$) gypsiric soils. Soils of SMU5, SMU4, and SMU3 have the highest gypsum contents ranging from 16.45 to 63.19% (Fig. 5).

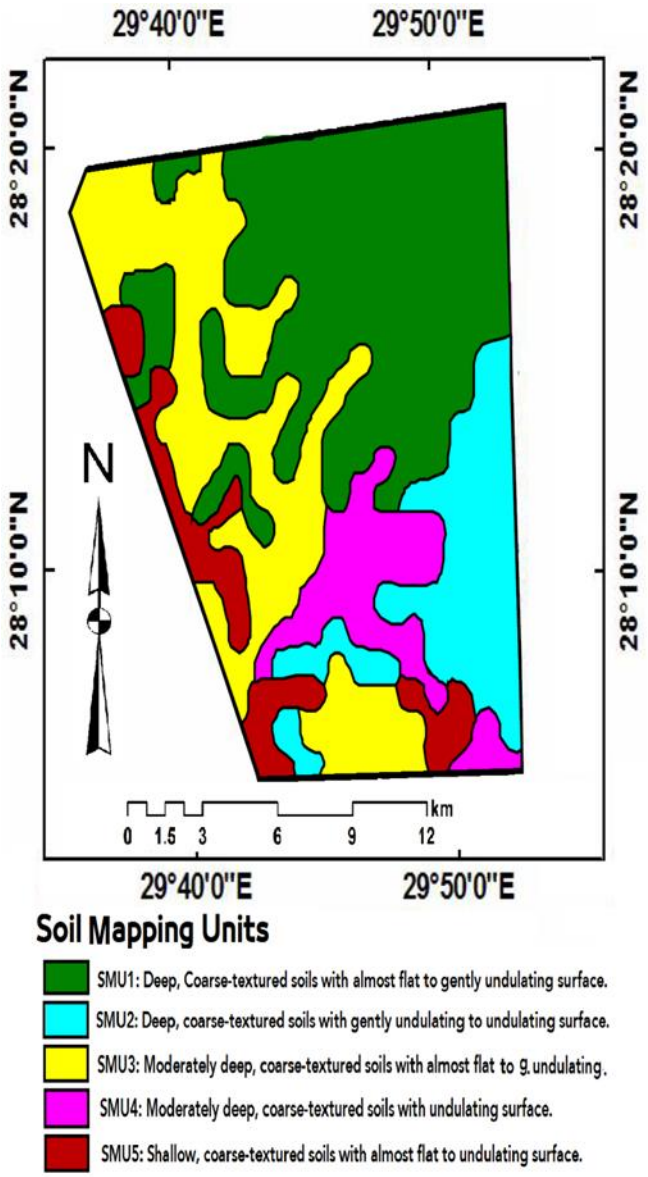

Fig. 4. Soil mapping units of the study area.

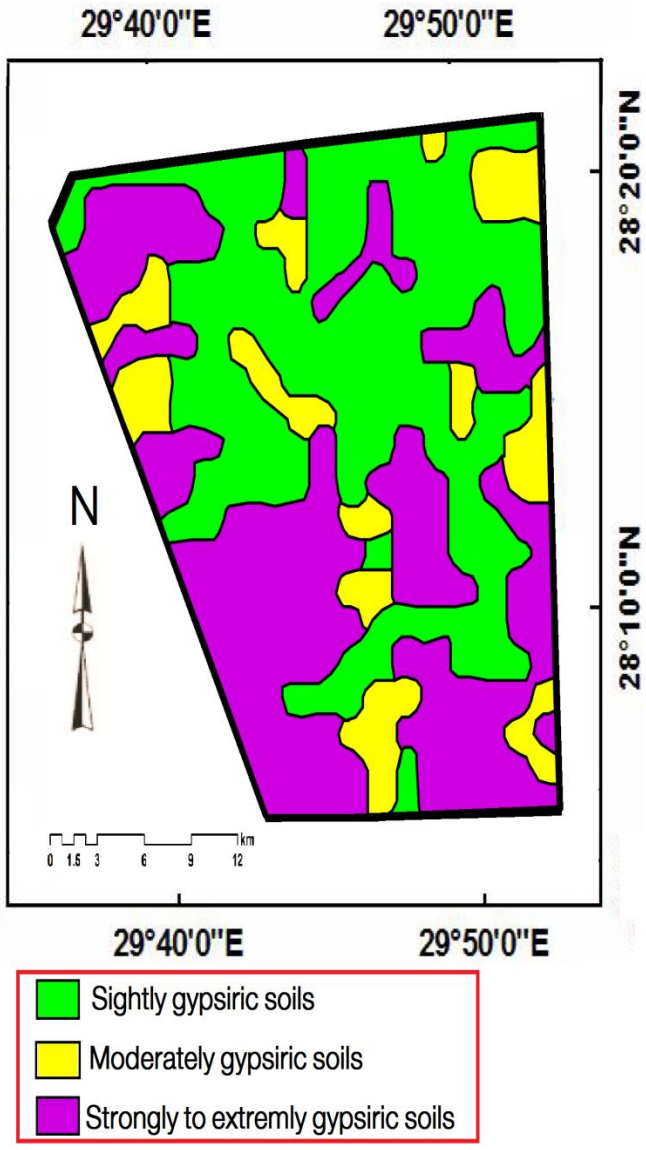

Fig. 5. Gypsum content in the studied soils.

In the investigated area, the surface horizon depth of the studied soils varies from 15 to 30 cm. These horizons have a yellow color with a value of more than 5 and a chroma of more than 4. Gypsum horizons were lighter in color and ranged from pinkish-gray (7.5 YR 7/2) in the C1 horizon of SMU 4 to white (7.5 YR 8/1) in the 2C1yy of SMU 3 (Table 2). The soil structureless was the dominant soil structure across soils of the toposequence transect, particularly soils derived from the limestone catena. The *gypsic* horizons (Cy & Cyy) exhibited a massive structure as well. The major morphological properties of sites and pedons of the study area are presented in Table (2) and visualized in Fig (6). The morphology of the studied soils on the lower slope differed from that of the gypseous soils on upland in their depth, colors, concentrations, redoximorphic features, and the absence or presence of diagnostic horizons/solum. The solum, the upper part of regolith (A+B horizons), was absent in the whole pedons whereas the subsolum layers; *e.g.*, regolithic layer (C), saprolithic (Cr), and paralithic layers (R), defined by Moragues-Quiroga et al., 2017, were noticed at different depths (Fig. 6). The regolithic layers (C) were the dominant horizons throughout the pedon. Furthermore, saprolithic (Cr), and paralithic layers (R) were only noticed in the deepest layers of the soils developed on higher slopes (Fig. 6). They were represented by a very pale brown (10YR 8/2) sand C layer, and light gray (10YR 7/2) sandy Cr layer.

The processes by which soil formation occurs are known collectively as pedogenic processes, and they comprise four main groups: additions, transformations, transfers, and losses (Elwan, 2018). Accordingly, there were noticeable differences in the horizon sequence between the pedons across the soil toposequence (Fig. 6). The investigated soils had different horizonation sequences: C-2Cyy for shallow soil in SMU5 developed on almost flat to undulating topography, C1-C2-2Cyy for moderately soils in SMU4 occurred on undulating topography, C-2C1yy-2C2yy for moderately soils in SMU3 developed on almost flat to gently undulating topography, C-Ck-2Cy-2Cr for deep soils in SMU2 developed on gently undulating to undulating topography and C-Ck-2C-3C for deep soils in SMU1 formed on almost flat to gently undulating topography surface (Fig. 6). The study demonstrated that the time wasn't adequate to develop the cambic horizon (Bw). Most soils were formed through geologic processes with no evidence of pedogenesis. Except for *calcic* horizons (Ck) formed on lower slope soils (SMU1 and SMU2), and *gypsic* horizons (2C1yy and 2C2yy) formed in upslope soils (SMU3, SMU4, and SMU5) ((Figs. 4 and 6).

In general, a soil texture group was only coarse-textured soils across the study area. In all studied pedons, the sand was a dominant fraction. Total sand content in the soil mapping units was higher (692-864 g kg^{-1}) compared to silt (89-232 g kg^{-1}) and clay (20-219 g kg^{-1}). The highest values of clay content were observed in the subsurface layers (2Cy and 2C) of the pedons sampled from SMU1 and SMU2. In contrast, pedons located upslope in the SMU4 and SMU5 present the highest sand content which may be attributed to the coarse sedimentary nature of the material from which upper positions sediments of the study area were formed. All soils consisted of Quaternary alluvial loamy coarse sand to sandy loam in deep (>100 cm) to shallow regolith (<50 cm) (Figs. 4 and 6).

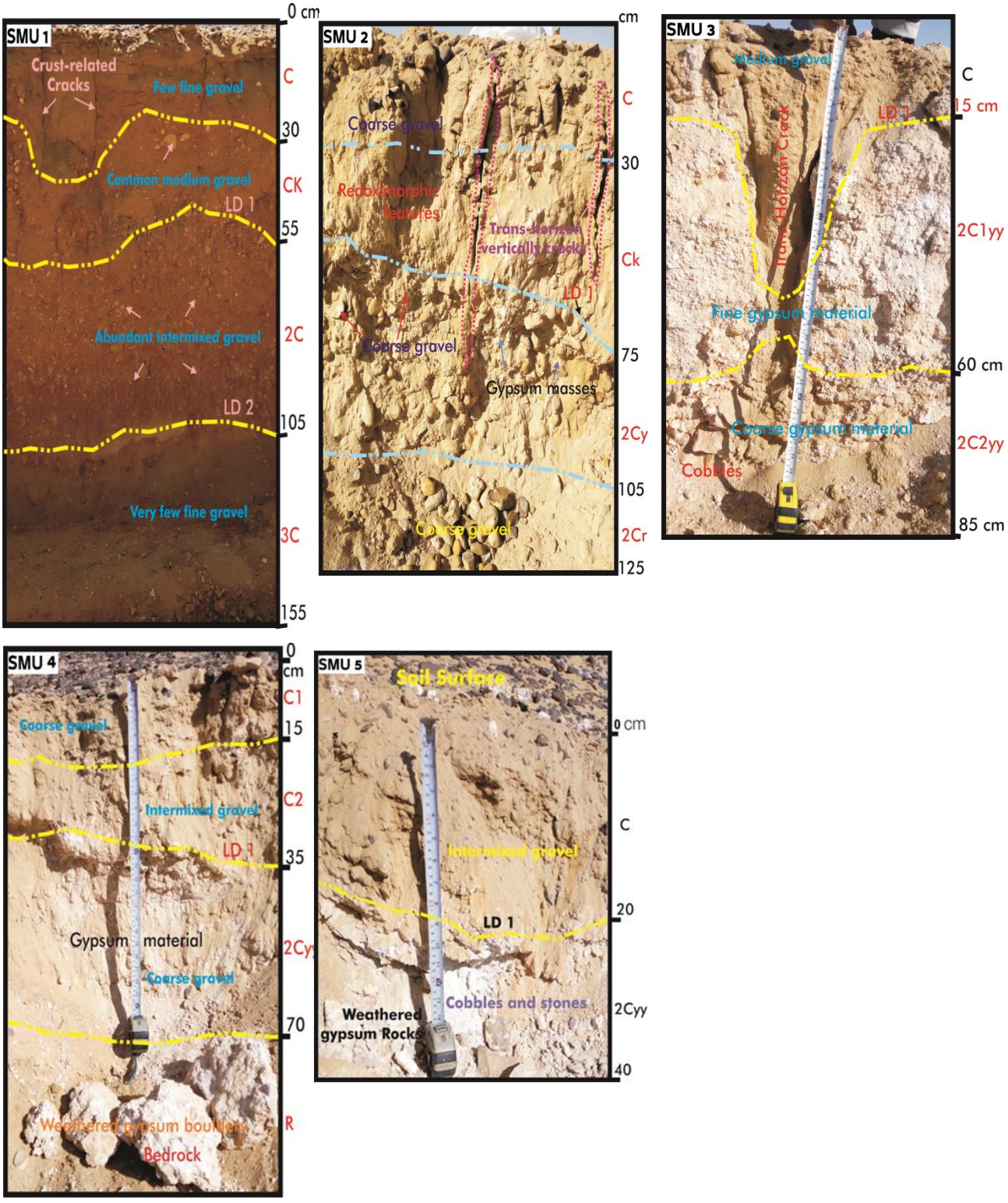

Fig. 6: Polygenetic reference pedons with different horizon sequences for the investigated soil types in West El-Minia, Central Egypt.

Table (1): Certain field morphological and physicochemical characteristics of the sampled pedons across the study area.

Pedon ID	Horizon	Layer thickness (cm)	Color†	Pedogenic features‡	Boundary§	$CaSO_4.2H_2O$ (%)	$CaCO_3$ (%)	Rock fragments (g kg^{-1})¶	Fine earth (g kg^{-1})¶			Sand separates (g kg^{-1})¶					USDA Texture¶	UV1#	UV2#
									S	Si	C	VCS	CS	MS	FS	VFS			
SMU1 (Deep soils)	**C**	0-30	7.5YR8/6	FDC	A,W	9.25	17.3	35	778	165	57	135	125	235	118	165	LCOS	-0.62	-0.44
	Ck	30-55	7.5YR8/4	FDC; F3M	A,W	3.15	39.5	95	699	210	91	135	98	359	95	12	SL	0.90	1.62
	2C	55-105	7.5YR7/8	FDC	A,S	9.7	14.6	590	721	135	144	103	125	215	189	89	LS	0.23	1.14
	3C	105-155	7.5YR7/6	F3M	--	4.15	19.7	15	637	215	148	208	139	107	111	72	COSL	--	--
SMU2 (Deep soils)	**C**	0-30	7.5YR8/3	F3M	A,S	4.17	21.75	175	864	92	44	305	209	197	139	14	LCOS	0.03	0.37
	Ck	30-75	7.5YR8/4	F3M	A,S	25.15	37.57	350	749	215	36	129	98	142	215	165	LS	0.95	0.52
	2Cy	75-105	7.5YR8/3	GYM,GNM	A,S	45.7	18.7	515	692	89	219	114	107	125	248	98	SL	-0.64	0.07
	2Cr	105-125	7.5YR8/4	F3M, FDG	--	11.6	15.5	410	706	221	73	129	145	59	162	211	LCOS	--	--
SMU3 (Moderately deep)	**C**	0-15	7.5YR6/8	FDC; F3M	A,B	19.45	7.5	150	730	210	60	79	145	214	117	175	SL	0.92	0.55
	2C1yy	15-60	7.5YR8/1	FDC, GNM	A,W	71.3	1.2	110	775	168	57	132	120	240	113	170	LCOS	-0.63	-0.44
	2C2yy	60-85	7.5YR8/2	GYM, FDG, GYX	--	59.5	1.9	375	855	91	54	239	215	311	56	34	COS	--	--
SMU4 (Moderately deep)	**C1**	0-15	7.5YR7/2	FDC, FDG	A, S	16.45	8.45	125	853	125	22	228	165	208	194	58	LCOS	-0.35	-0.55
	C2	15-35	7.5YR7/3	GYM, FDG	A,W	42.9	5.48	875	727	231	42	210	98	157	176	86	COSL	0.87	-0.02
	2Cyy	35-70	7.5YR8/2	GYM, GNM, GYX,	--	50.48	2.19	370	847	133	20	209	199	247	106	86	LCOS	--	--
SMU5 (Shallow)	**C**	0-20	7.5YR8/4	FDC, FDG	A,W	27.45	9.48	145	742	136	122	205	124	217	89	107	COSL	-0.65	-0.07
	2Cyy	20-40	7.5YR8/2	GYM, GNM, GYX	--	63.19	1.57	250	741	232	27	105	240	191	153	52	LCOS	--	--

Explanations: † 7.5YR 8/1 (white), 7.5YR 8/2 (pinkish white), 7.5YR 8/3, 7/3 , 8/4 (pink), 7.5YR 7/2 (pinkish gray), 7.5YR 6/6, 6/8, 7/6, 7/8, 8/6 (reddish yellow); ‡ FDC (finely disseminated carbonates), CAM (carbonate masses), CAC (carbonate concretions), GYM (noncemented gypsum masses), FDG (finely disseminated gypsum), GNM (gypsum crystal clusters (nests) very fine crystals), GYX (Visible gypsum crystals), F3M (F^{3+} masses), §A (abrupt), S (smooth), W (wavy), B (broken); ¶ Rock fragments (>2000 µm), S = sand (2000->63 µm), Si = silt (63-2 µm), C = clay (<2 µm), VCOS = very coarse sand (2000->1000 µm), COS = coarse sand (1000->500 µm), MS = medium sand (500->250 µm), FS = fine sand (250->125 µm), VFS = very fine sand (125->63 µm), LCOS (loamy coarse sand), COSL (coarse sandy loam), LS (loamy sand), SL (sandy loam); # UV1 (uniformity value index of Cremeens and Mokma, 1986), UV2 (uniformity value index of Kowalska et al., 2016).

Gypsum ($CaSO_4.2H_2O$) and lime ($CaCO_3$) contents are related to the kind of parent material and slope position. Gypsum content was observed in soils of SMU1, SMU2, and SMU3 at lower slope positions while it was absent in soils of SMU1. Soils of the study area were categorized into three classes based on gypsum concentration (Fig. 5). The highest gypsum values (>60% $CaSO_4.2H_2O$) were recorded in *gypsic* horizons (Cyy) and the lowest values (<5% $CaSO_4.2H_2O$) were recorded in *calcic* horizons at lower slopes in SMU1 and SMU2. In comparison, $CaCO_3$ content was higher in the lower positions at SMU1 and SMU2 ranging from 14.6% (strongly calcareous) to 39.5% (extremely calcareous) (FAO, 2006). While the slightly calcareous sediment (<2%) occurred only in the *gypsic* horizons (Cy and Cyy) within the pedons of SMU4 and SMU5. Pedons from the third mapping unit (SMU3), except the surface layer, are slightly affected by the calcareous nature compared with other soil mapping units. The laboratory data were found to be consistent with the morphological description, showing parallels to the $CaCO_3$ and gypsum contents. The concentrations of secondary lime, gypsum, and iron masses were the most pedogenic characters in the pedons (Table 2). Accumulation of secondary carbonate (SMU1 and SMU2) and gypsum (SMU3, SMU4, and SMU5) qualifies as *calcic* and *gypsic* horizons, respectively (Figs. 4, 5, and 6).

The gypsification and calcification are the major processes that occurred in studied soils across the toposequence transect. The calcification process was mainly present on limestone catena and gypsification, a generalized process in gyprock catena (Figs. 4, 5, and 6). The incipient secondary carbonate accumulations within subsurface horizons allowed to designate of a *calcic* horizon in the lower slope profiles in SMU1 and SMU2, suggesting some oblique and vertical leaching along the slope gradient. Secondary carbonate pedofeatures were registered as small and thin pendants within gravel in Ck horizons. *Calcic* horizons were a common feature of submature soils in the studied area. Studied soils from the gypsum catena are characterized by significant accumulations of pedogenic gypsum. Cy-horizons of soils from higher slopes contain enough gypsum to qualify the profile as gypsisols group and therefore *hypergypsic* (>50% gypsum content). The gypsum materials have a flour-like consistency of silt-sized crystals in the field. Furthermore, infillings in pore spaces, with a powdery consistency in the field, are composed of sand-sized lenticular gypsum that appears as faint gray and bright crystals (Figs. 4, 5, and 6).

Lithologic discontinuities and soil uniformity

Genetic horizon boundaries provide information on the dominant soil-forming processes that have formed the soil (FAO, 2006) while layer boundaries provide evidence for the past geogenic processes. Evidence cited for LD sharp, abrupt, smooth, and wavy boundaries. Boundaries between C layers in studied pedons are varied in both distinctiveness and topography. Abrupt smooth boundaries were the dominant within the most investigated pedons (Figs. 4 and 6; Table 1). The occurrence of smooth to broken and abrupt to diffuse boundaries in studied pedons is often cited as field evidence for the LD (Schaetzl and Anderson, 2005; Soil Survey Staff, 2014a). Abrupt smooth C1-C2 boundaries occurred only in upper layers of SMU4 pedons that have the same geological parent material. In the lower horizons in the same pedons, the soil exhibited abrupt wavy C2-2Cyy boundaries indicating two unlike parent materials with different modes of deposition The boundary investigations advocated that the layer/horizon boundaries in studied pedons failed to detect the real LDs in soils. This may be attributed to the boundary between two layers being identified based on color, texture, structure, hardness, or other features which largely influenced by the pedogenic process. Consequently, the horizon/layer boundary was a very poor morphologic indicator for detecting LDs in studied soils.

Based on the field observations, the coarse fragments tend to be distinctive to LD. Lamina (geogenically deposited strata or layers of alternating texture) were the most geologic features recorded in the upper layers of most studied pedons (Table 2). The visual estimation of rock fragments showed abrupt changes vertically within the pedon layers which were not resulting from pedogenic processes. Accordingly, LDs are often indicated by an erratic distribution of rock fragments within the investigated pedons. Most studied pedons of the toposequence, especially in SMU2, have coarse fragments content exceeding 150 g kg^{-1}. In comparison, pedons in the lower positions (P7, P10, and P16) have less than 150 g kg^{-1} coarse fragments content (Table 2). The microcrystalline quartz (chert) was abundant within SMU2 layers indicating one LD at 75 cm (Fig. 6). It is a natural concentration of rock fragments (chert) caused by water erosion or transport erosional lag (Schoeneberger et al., 2012). The material (Cy) above the stone line is most likely transported, and the material below may be of different origins (Soil Survey Staff, 2014a). This observation represents different mechanisms of transport (colluvial, aeolian, and alluvial) with different transport distances (Table 1). The occurrence of LDs was proven using the uniformity indices (UV1, UV2) (Table 1). The difference in sand and silt separates of UV1 on a carbonate-free and clay-free basis was consistent with the vertical distribution of rock fragments

within the pedon (Table 1). Accordingly, an abrupt change in particle size distribution (PSD), which is not resulting from pedogenesis, was observed in most studied pedons that have high values of UV1. Hence, the analyzed pedons were considered LDs. The observed differences in UV1 between the different layers were greater than 0.60. By contrast, the UV2 values were less than 0.60 (Table 1) in most of these pedons indicated no differences in the pedon materials which are not consistent with the morphological indicators (*e.g.*, inverse distribution of rock fragments and stone line). The lower values of UV2 observed in most studied pedons indicate the limitation of this method which failed to estimate the uniformity of parent material. Distinct breaks in the lithology of soils can occur in two ways: geologically-sedimentologically or pedologically. The contact between two, unlike parent materials, is called a lithologic discontinuity (LD) (Elwan, 2018). LDs provide important information on parent material origins and subsequent pathways of soil development (Cámara et al., 2017) (Figs. 4, and 6). They represent zones of change in the lithology of soil parent materials that are interpreted to be primarily lithologic, rather than pedogenic (Schaetzl and Anderson, 2005; Cámara et al., 2017). Abrupt changes in sedimentation were found across the studied transect sediments to indicate the LDs via the grain-size composition of the whole soil, including both the fine earth (silt and sand) and the rock fragments. Many pedons in the study area have formed in more than one parent material, however, the UV2 values within the most investigated pedons were less than 0.60, indicating homogeneity of parent materials which are the erroneous results because the pedogenic processes may cause translocation of the clay fraction (Fig. 4). By contrast, the UV1 had values greater than 0.6, indicating multiple parent material. At the same time, this heterogeneity within these pedons was further approved by the vertical distribution of coarse fragments. Therefore, the UV2 of Kowalska et al. (2016) produced erroneous results and failed to reveal LD vertically within soils under study.

The presence of LD in most studied pedons was not a result of standard soil-forming processes, but usually the result of geogenesis. To be even more discriminatory, the identification of a geologic LD should be based on data from an immobile and slowly weatherable soil fraction (Schaetzl and Anderson, 2005). Immobile elements used in UV1 of Cremeens and Mokma (1986) are excellent indicators of LDs because they reflect sedimentology better than do mobile, or plasma, and particles < 2 µm as used in the UV2 method. Hence, the use of the UV1 method to determine LD constitutes a pioneering approach to LD detection while the UV2 method is the improper method to reflect the real LD, and consequently, it is not recommended by this study. Moreover, coarse fragments abundance vertically within the pedon indicated the presence of an erosional episode and thus can detect any LD (Fig. 6; Table 1). Accordingly, the clay-free basis indices (*e.g.*, UV1 and rock fragments as a morphologic indicator) are recommended by the author to detect a clue to a lithologic change in, unlike parent materials.

The distribution curves of weathering ratios (Wr1, Wr2, and Wr3) as a function of depth for the studied soils are drawn in Fig. 7. The curves showed a similar trend with a smooth shape without inflection in some adjacent layers, but a different trend across the whole pedon (Fig. 7). This trend indicates parent material uniformity for the neighboring layers and heterogeneity for the whole pedons. In the SMU1 pedon, the weathering ratios depth distribution curves (Fig. 7) had an inflection suggesting a change of materials vertically within the. The depth distribution curves in fine earth fractions indicate an inflection at 55 cm depth of the Ck horizon (Figs. 6 and 7).

Light Minerals

The light mineral associations in the studied soils were dominated by quartz, feldspars, calcite, mica, chlorite, and gypsum (Table 2). The percentages of quartz (SiO_2) varied from 19.5% in shallow soils at a high elevation of the soil transect to 63.27% in deep soils at a low elevation of the toposequence (SMU1). There is either no regular trend of percent variation or, if any, an increase with the increase of distance from the east to the west (Table 3 and Figs. 5 to 7). Feldspars, $(Na, Ca)(Si,Al)_4O_8$, content range from 3.15% (SMU) to 25.65% (SMU2) with an average value of 43.4% (Table 2). Regarding the variations of feldspars across the toposequence transect, it is obvious that they slightly decrease in samples located away from the limestone plateau (Table 2). Calcite (carbonate minerals, $CaCO_3$) was recorded in all soil samples studied with varying frequencies. The percentage values of calcite mineral range from 3.15% (In samples close to the high slope) to 22.45% in deep soils of lower slopes. Mica, $KA_{l2}(Si_3Al)O_{10}(OH,F)_2$, minerals are generally present in small amounts. It varies from 1.54 in *gypsic* horizons to 8.65% in *calcic* horizons. Chlorite, $(Mg, Fe, Li)_6AlSi_3O_{10}(OH)_8$, Also, chlorite mineral is present in small amounts in the examined soil sediment samples. However, its content is higher and ranges from 0.25% to 5.1%.

The interplay of moisture and temperature is a major factor in determining soil characteristics (Woodruff et al., 2015), and the flooding effects are strongly imprinted on the distribution of many elements and minerals across the soil transect. One of the most fundamental changes in soil composition across the study area is the weathering of feldspar in soil along the gradient of increased

precipitation from the east of the plateau to the west of the study area. Feldspar minerals are very reactive in the soil environment, typically breaking downslope by hydrolysis and leaching to form the clay mineral kaolinite while releasing Ca, Na, or K cations into the solution. Feldspar, prevalent in the soil, sourced from metamorphic and igneous rocks gives way to the soil in SMU1 formed from similar parent materials from which the original feldspar has been largely obliterated by weathering (Yang et al., 2018). These soils are moderately weathered and most feldspar may be altered to Al-rich clay (Woodruff et al., 2015). This loss of feldspar in the soil is expressed not only mineralogically by the transformation of feldspar to kaolinite and then to gibbsite (Yang et al., 2018), but chemically in the leaching of nearly all major and trace elements present in the feldspar structure (Woodruff et al., 2015).

Heavy Minerals and Provenance Discrimination

Heavy mineral percentages by weight increased across the slope gradient (1.46 – 16.34%), with a marked transition from the upper to the lower slopes (Table 3). They increased with decreasing elevation from the west to the east. The highest concentration of heavy minerals (10.09 – 16.34%) was detected in the lower soils of SMU1. The increasing trend may be ascribed to the deposition of stable heavy minerals from upper slopes and surrounding lithology. The distribution of heavy mineral characteristics in the sediments of the studied transect is related to the type of lithology rocks. The identified heavy minerals were pyroxene (augite and hyperthene), amphiboles (hornblende and actinolite), garnet, staurolite, kyanite, zircon, tourmaline, rutile, epidote, zoisite, biotite, monazite, glaconite, and opaques. This heavy minerals assemblage varied from ultrastable to very unstable minerals (Table 3). Olivine, hornblende, and augite show a descending trend from the higher slope to the lower slope, whereas epidote, zircon, rutile, and tourmaline show an increasing trend at the downslope. Opaque minerals constitute the most predominant constituent in all studied soil samples. They range from 39.33 to 60.33% across the studied toposequence transect. On the other hand, no clear trends of variations in such minerals could be noted in the study area. Amphiboles, (Na, Ca, Mg, Fe, $Al)_{7\text{-}8}(Al, Si)_8O_{22}(OH)_2$, range from 1.92 to 34.53%. Thus, it can be stated that the percentage of amphiboles generally increases from the west at higher slopes to the east at lower slopes. It has been observed that a fair concentration and several heavy minerals species have been recorded from the sediments of the study area (Table 3). The heavy minerals assemblage across the toposequence varied with lithology structure and landscape position.

In soils of SMU4 and SMU5 at high slopes of the studied toposequence, opaques (56.45 – 61.33%), hornblende (0.23 – 8.45%), zircon (1.54 – 9.31%), rutile (1.04-6.24%), tourmaline (2.34 – 6.75%), biotite (19.56 – 37.32%), and monazite (1.58 – 12.11%) were recorded as the dominant heavy minerals. Sediments from lower slopes in SMU1 and SMU2 were dominated by opaques (39.33 – 61.33%), hornblende (11.89 – 33.21%), biotite (1.17 – 35.12%), kyanite (1.21 - 21.65%), zircon (2.19 - 12.26%), garnet (0.25 - 11.45%), epidote (0.05 - 11.24%), tourmaline (1.35 - 13.65%), rutile (2.36-11.74), monazite (2.89 - 9.31%), staurolite (1.21 - 9.25%), zoisite (1.25 - 7.25%), and olivine (0.34 - 5.08%) (Table 3). High concentrations of epidote, kyanite, zoisite, garnet, and staurolite were found in soils of SMU1. The highest concentration of hornblende (11.89 – 33.21%) was recorded in SMU1 and SMU2, and the lowest concentration (0.23 – 8.47%) was found in soils at upper slopes, i.e., SMU3, AMU4, SMU5 which may be attributed to its instability and the rapid erosion from upslope to downslope. Other important but minor heavy minerals were detected with traces of monazite, glaconite, kyanite, and zoisite.

Based on heavy minerals, an attempt has been carried out to find out their parent rock's provenance (Moragues-Quiroga et al., 2017; Sulieman et al., 2021). Some of the heavy minerals are diagnostic of a particular source rock type such as garnet, kyanite, zoisite, and staurolite for high-rank metamorphic rock; biotite, hornblende, and monazite for acid igneous rock; augite, olivine, and augite for basic igneous rock. The non-opaque mineral assemblage consists of ultrastable minerals (e.g., zircon, tourmaline, and rutile), stable minerals (e.g., garnet, staurolite, biotite, and monazite), moderately stable minerals (e.g., epidote, kyanite, and zoisite), unstable minerals (e.g., hornblende and augite), and very unstable (e.g., olivine).

The results of weathering indices are presented in Table (3) and visualized as curves in Fig. (7). They showed that the soils under study are formed from multi-origin under multi-depositional regimes. To demonstrate uniformity or discontinuity of parent material, the weathering indices were performed by stratifying the ratios of Wr1, Wr2, and Wr3. The results exhibit that uniformity ratios have irregular distribution with depth in all the studied soil profiles. Correspondingly, soil parent materials of each profile are heterogeneous and formed of multi-depositional regimes (Fig.7). In general, data of uniformity ratios gravitate to boost the existence of lithological discontinuities specified by field morphology. Although the limestone plateau was the main source of soil regolith, the uniformity

ratios depict heterogeneous distribution with depth that may be due to the sedimentation processes which act upon most soils. Few exceptional cases are detected in some soil profiles where pairs or three adjacent layers are of homogenous parent materials. The maturity ZTR index exhibited a relatively wide range of values ranging from 11.89% in higher slope soils to 74.54% in lower slope soils. The lower values of the ZTR index (<40% ZTR) suggest that the majority of soils contain mineralogical immature sediments except for limited locations at the lower slope position which have > 50% indicates submature sediments (Table 3; Fig. 7).

Table (2): Composition of light minerals in the fine sand portion (63-250 μm) along the soil gradient transect.

Pedon ID	Horizon/Layer	Basal depth, cm	Altitude (above sea level, m)	Quartz	Feldspar	Calcite	Mica	Chlorite	Gypsum	Others
SMU1	**C**	**30**	135 m	63.27	7.35	15.7	2.4	1.6	9.5	0.18
	Ck	**55**		62.13	3.15	22.45	5.1	2.9	1.65	2.62
	2C	**105**		53.25	7.8	15.6	3.25	1.5	5.06	13.54
	3C	**155**		61.15	5.5	13.4	1.7	1.9	13.41	2.94
SMU2	**C**	**30**	125 m	54.1	9.6	19.8	3.3	5.1	5.48	2.62
	Ck	**75**		53.5	7.4	11.01	7.05	4.25	10.17	6.62
	2Cy	**105**		59.65	9.15	7.54	6.1	2.78	13.25	1.53
	2Cr	**125**		50.32	19.45	10.25	5.14	1.25	9.08	4.51
SMU3	**C**	**15**	115 m	44.65	23.65	9.59	4.45	2.36	6.45	8.85
	2C1yy	**60**		41.45	9.45	2.45	2.65	1.14	39.4	3.46
	2C2yy	**85**		32.05	13.65	3.15	1.45	2.59	45.07	2.04
SMU4	**C1**	**15**	105	43.15	25.65	4.15	8.65	2.45	13.08	2.87
	C2	**35**		41.54	20.35	5.47	3.4	3.5	22.45	3.29
	2Cyy	**70**		21.45	15.62	3.45	2.9	1.98	51.35	3.25
SMU5	**C**	**20**	95	41.35	19.45	7.65	2.15	3.25	21.5	4.65
	2Cyy	**40**		19.5	13.25	3.45	1.54	0.25	55.9	6.11

Table (3): Distribution of heavy minerals in the fine sand fraction (63-250 µm) of soils along the studied toposequence.

Pedon ID	Depth, cm	Horizon /Layer	HF	Opq	Non-Opaques														Weathering Indices			ZTR Index
					Pyroxine		Amphiboles		Ga	St	Ky	Zi	R	T	Ep	Zios	Bio	Mo	Gl	Wr1	Wr2	Wr3	
					Au	Hy	Ho	Act															
SMU1	0-30	C	13.17	45.44	6.65	1.21	22.22	3.21	0.32	1.34	0.23	12.32	9.43	12.12	7.46	7.24	13.34	1.02	1.89	1.36	0.91	0.55	74.54
	30-55	Ck	10.09	57.77	8.67	3.87	33.21	1.32	2.32	1.32	0.00	7.55	13.43	14.32	3.34	4.32	4.00	2.33	0.00	2.15	1.52	0.18	61.10
	55-105	2C	16.34	39.33	7.65	4.23	11.89	0.98	1.90	5.54	2.56	5.34	14.98	3.23	4.23	2.23	35.12	0.12	0.00	2.89	1.39	4.10	59.88
	105-155	3C	14.01	55.33	15.78	6.98	21.29	7.32	0.00	2.13	0.65	9.32	12.87	9.15	9.22	1.56	1.17	2.02	0.54	2.78	1.15	0.06	56.64
SMU2	0-30	C	15.90	47.35	9.87	4.98	10.43	1.78	9.21	5.32	1.88	15.12	11.23	2.21	5.36	1.24	11.21	9.12	1.04	1.56	0.60	0.65	60.32
	30-75	Ck	9.56	61.33	5.55	2.60	15.22	3.21	1.20	1.32	0.45	9.22	14.56	5.43	10.34	3.43	20.62	3.45	3.40	1.81	1.04	1.41	47.63
	75-105	2Cy	12.89	39.66	7.85	3.98	14.45	2.43	5.40	1.98	0.89	7.34	13.54	0.00	3.32	2.40	28.22	2.45	5.75	3.91	1.97	3.84	52.65
	105-125	2Cr	11.84	53.22	13.56	3.49	18.78	1.34	0.00	3.43	2.21	10.34	12.34	3.20	4.32	3.21	21.78	1.25	0.75	2.75	1.39	1.61	48.63
SMU3	0-15	C	15.13	56.53	34.34	2.25	7.11	3.32	2.00	3.87	0.76	6.44	15.09	9.34	0.35	1.23	11.45	2.45	0.00	2.98	0.45	0.73	54.61
	15-60	2C1yy	8.12	48.22	26.67	1.98	1.88	0.37	3.87	2.65	1.23	3.23	1.23	4.50	3.34	0.09	45.51	2.45	1.00	4.00	0.24	5.89	18.58
	60-85	2C2yy	6.89	40.22	42.71	1.98	0.52	4.34	4.34	1.34	2.53	7.34	7.24	11.43	9.34	0.67	5.77	0.45	0.00	2.64	0.03	0.31	64.67
SMU4	0-15	C1	2.77	60.33	10.32	11.67	1.47	0.45	5.32	1.98	5.43	9.31	1.23	6.75	8.34	1.78	24.85	9.55	1.55	1.49	0.09	1.55	28.66
	15-35	C2	4.57	56.45	6.47	10.98	8.45	4.23	6.35	3.48	7.09	1.54	4.32	4.32	1.35	1.23	27.03	12.11	1.05	5.14	1.44	4.61	18.03
	35-70	2Cyy	3.46	57.87	10.21	12.80	1.44	3.20	9.12	2.34	5.12	5.56	6.24	5.33	2.11	1.23	19.56	10.54	5.20	2.54	0.13	1.80	29.60
SMU5	0-20	C	5.78	57.56	17.32	1.98	0.23	9.45	9.20	2.67	3.86	7.67	5.43	2.34	0.23	3.24	33.78	1.58	1.02	2.90	0.02	3.37	26.82
	20-40	2Cyy	1.46	56.43	15.11	6.20	2.78	11.12	4.20	5.34	4.88	2.23	1.04	3.44	1.87	2.12	37.32	2.35	0.00	6.21	0.49	6.58	11.89

Explanations: † HF (heavy mineral fraction); ‡Opq (Opaques); §Au (Augite), Hy (Hyperthene), Ho (Hornblend), Act (Actinolite), Ga (garnet), St (staurolite), Ky (kyanite), Zi (zircon), R (rutile), T (tourmaline), Ep (epidotes), Zios (Ziosite), Bio (Biotite), Mo (monazite), Gl (Glaconite); ¶ Wr1= (Pyroxene + Amphiboles) / (Zircon + Tourmaline), Wr2= Hornblend /(Zircon + Tourmaline), Wr3 = Biotite /(Zircon + Tourmaline). ZTR ([(zircon+tourmaline+rutile)/(Σ non-opaques)] × 100).

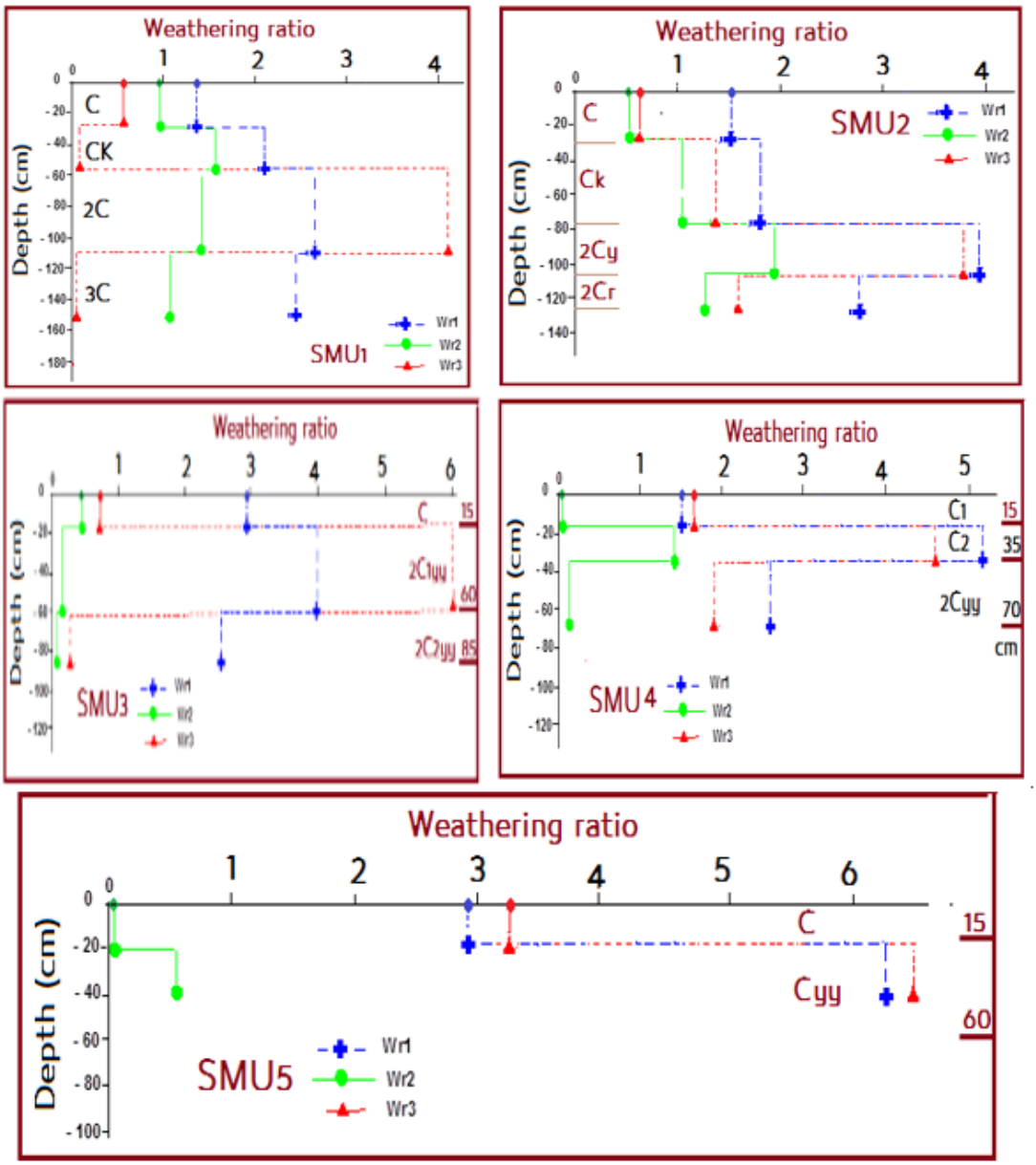

Fig. 7. The depth distribution curves of the weathering indices in the studied soils across soil mapping units.

The Genesis of Gypsum-enriched Soils

Based on data of the field morphology studies and physicochemical characteristics of soils given in Table (1) and visualized in Figs. (5, 6, and 8), the developmental genetic stages of *gypsic* horizons horizontally across the toposequence transect and vertically within the soil pedons were suggested. The first stage includes gypsum accumulation in the studied soils and was commenced by transporting the geologic gypsum sediments from the rock gypsum of the surrounding plateau through runoff forming the soils of the coarse-textured material at upper positions. Then, the gypsum lenticular crystals were deposited and formed in fine pores of soil voids by following evaporation processes (Figs. 6 and 8). Soil structureless of a single grain in studied coarse-textured soils with loose consistency causes the growth of gypsum crystals within the horizons of studied pedons. Furthermore, some gypsum crystals have occurred within other forms than the void of soil horizons. The gypsum content of developed soils under this stage was not exceeding 5% $CaSO_4.2H_2O$. The gypsum crystals were visually observed in the studied pedons during the field survey. In the second stage, the gypsum crystallization was continued and increased in terms of the colonies, size, and number of gypsum crystals which were visually noticed in the gypsum materials within soil pedons. Lenticular crystals of

gypsum were slightly formed within the soil groundmass but the soil regolith remains structureless massive. The gypsum crystal nests have not been connected in this stage and the criteria for *gypsic* horizon to be developed are not met. In the third stage, the regolith materials are finer at middle or lower slope positions of the toposequence transect and therefore the gypsification processes were more active. Increasing the size and amount of crystals causes the formation of granules, internal coating of channels and chambers, infillings, and pendants. In this stage, gypsum spots and little pendants may be observed in the field. The soil in this stage meets *gypsic* horizon criteria and the amounts of gypsum range from 15% to more than 50%. The fourth stage includes the formation of *hypergypsic* horizons within the regolith layers. The lower slope positions in the studied lands are characterized by dissected surfaces and gravelly plain. Gypsum materials were received from the late Pleistocene or early Quaternary and deposited in these radial slope positions by flooding and continued runoff therefore the soil surfaces have complicated pedofeatures due to the high enrichment with gypsum. The *gypsiferous/gypseous* soils were gradually formed by arranging the gypsum crystal in different shapes and various distributions through runoff water. The soil groundmass in this stage consists mostly of lenticular *gypsic* crystallites and isles fabrics. These criteria soils meet all *hypergypsic* requirements. Where these soils have a gypsum substitute of 40 percent or more (by weight) gypsum in the fine-earth fraction that replaces the particle-size class in the mineralogy control section. Lenticular crystals were vertically arranged and formed as a result of the continuous evaporation of water. Therefore, new gypsum crystals are recrystallized along with the other recrystallized gypsum within the horizons of soil pedons. Then the gypsum fibers and gypsum pendants were eventually developed underneath the gravel across soil pedons. A crystalline network of porous media of gypsum was established through the connection of some gypsum pendants in these gravelly soils that construct the whole pedon. The formation of lenticular gypsum crystallites and isles fabrics is the result of these processes. These soils were classified as a *hypergypsic* based on the soil morphology and physicochemical data and soil taxonomic manuals. Three important geochemical processes of gypsum formation were oxidation of sulfide minerals, hydration of anhydrite, and direct deposition from an evaporating solution saturated with gypsum. Looking at the different probable mechanisms of gypsum formation mentioned above, the evaporation from solutions saturated with $SO4^{-2}$ was the major mechanism for gypsum accumulation in the soils of the study area. The origin and genesis of *gypsic* and *hypergypsic* horizons were proved. Gypsum materials in studied soils originated mainly from the weathering of the Eocene white limestone of the surrounding plateau sediments.

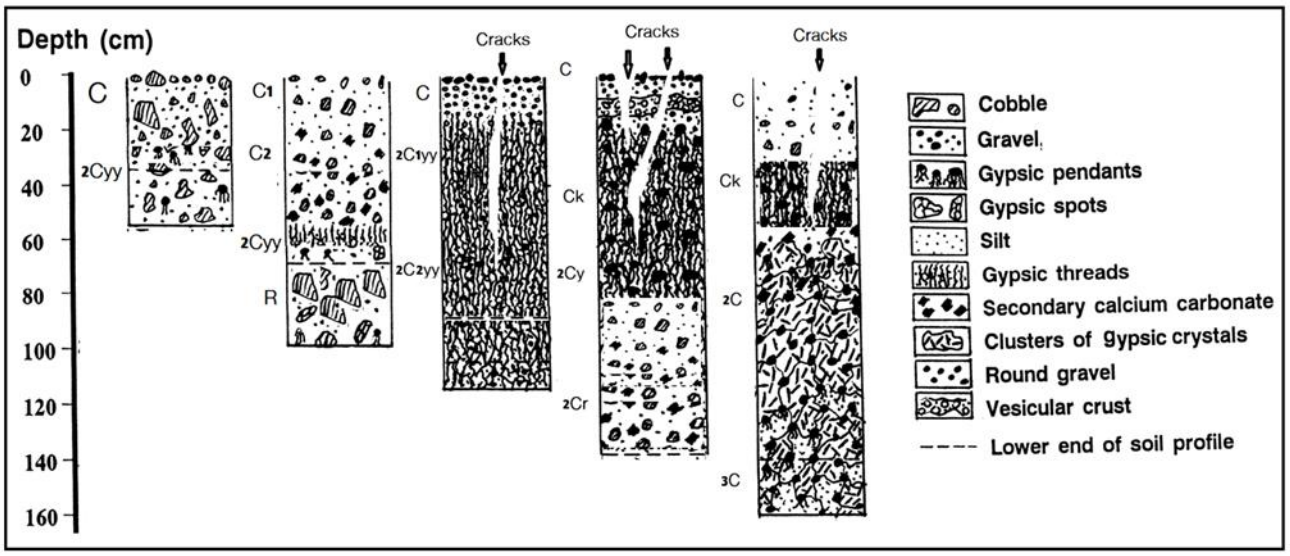

Fig. 8. Horizonation sequences of representative studied pedons across studied soil mapping units.

The soils across the toposequence of 95-135 m were investigated at the Darb Al-Bahnsawy area, West El-Minia, Central Egypt for identifying the origin and uniformity of the soils under study. Five soil mapping units were identified according to soil depth, soil texture, and surface topography. The investigated soils were coarse-textured and widely varied from deep (>100cm) to shallow (<50 cm). The studied soils were highly impacted by gypsum accumulations and ranged from slightly gypsiric to extremely gypsiric soils. The soils were also affected by the calcareous nature and the *calcic* horizons were formed in lower slope soils. *Calcic* horizons (Ck) were formed on lower slope soils, while the *gypsic* horizons such as 2C1yy and 2C2yy were formed on upslope soils along the toposequence transect. Lithologic discontinuities were studied using the uniformity indices of UV1 and UV2 and weathering indices of Wr1, Wr2, and Wr3. This suggested sequences of deposition and erosion processes and the heterogeneity of the parent material. The identified heavy minerals were dominated by pyroxene (augite and hyperthene), amphiboles (hornblende and actinolite), garnet, staurolite, kyanite, zircon, tourmaline, rutile, epidote, zoisite, biotite, monazite, glaconite, and opaques. The heavy minerals characteristics suggest their mixed sources from sandstone, limestone, and metamorphic rocks. Limestone plateau was the main source of soil regolith, the uniformity ratios depict heterogeneous distribution with depth that may be due to the sedimentation processes which act upon most soils. The maturity ZTR index ranged from 11.89% in higher slope soils indicating immature sediments to 74.54% in lower slope soils indicating submature sediments. The developmental genetic stages of *gypsic* horizons horizontally across the toposequence transect and vertically within the soil pedons were suggested. The origin and genesis of *gypsic* and *hypergypsic* horizons were proved. Gypsum materials in studied soils originated mainly from the weathering of the Eocene white limestone of the surrounding plateau sediments. In general, data of uniformity ratios gravitate to boost the existence of lithological discontinuities specified by field morphology. Although the limestone plateau was the main source of soil regolith, the uniformity ratios depict heterogeneous distribution with depth that may be due to the sedimentation processes which act upon most soils. The results of Wr1, Wr2, and Wr3 exhibited that uniformity ratios have irregular distribution with depth in all the studied soil profiles. Correspondingly, soil parent materials of each soil pedon are heterogeneous and formed of multi-depositional regimes.

REFERENCES

Abu-Bakr, H.A., 2020. Groundwater vulnerability assessment in different types of aquifers. Agricultural Water Management 240, 106275.

Artieda, O., Herrero, J., Drohan, P., 2006. Refinement of the differential water loss method for gypsum determination in soils. Soil Sci. Soc. Am. J., 70(6): 1932–1935.

Baillie, I.C., Floyd, C.N., Hallett, S.H., Andrews, R., 2021. Topographic zonation and polycyclic pedogenesis in the northern atolls of the Chagos Archipelago, Indian Ocean. Geoderma Regional 26, e00391.

Bockheim, J.G., Gennadiyev, A.N., Hammer, R.D., Tandarich, J.P., 2005. Historical development of key concepts in pedology. Geoderma 124, 23–36.

Cámara, J., Gómez-Miguel, V., Martín, M. A., 2017. Lithologic control on soil texture heterogeneity. Geoderma, 287: 157-163.

Cremeens, D. L., Mokma D. L., 1986. Argillic horizon expression and classification in the soils of two Michigan hydrosequences. Soil Sci. Soc. Am. J., 50: 1002-1007.

El-Rawy, M., Moghazy, H.E., Eltarabily, M.G., 2021. Impacts of decreasing Nile flow on the Nile Valley aquifer in El-Minia Governorate, Egypt. Alexandria Engineering Journal, 60, 2179–2192.

Elwan, 2018. Formation and Taxa of some Wadi Dahab Tributaries Soils, South Sinai, Egypt. Journal of Soil & Water Sciences; Suez Canal University. 4 (1): 27-48.

FAO, 2006. Guidelines for Soil Description. fourth ed., pp. 1-98 Rome.

IUSS Working Group WRB, 2015. World Reference Base for Soil Resources 2014, update 2015 International soil classification system for naming soils and creating legends for soil maps. World Soil Resources Reports No. 106. FAO, Rome.

Kapur, S., Costantini, E., Kadir, S., Zucca, C., Stahr, K., 2018. A tribute to Ewart A. FitzPatrick (1926–2018), a life for Pedology and Morphology of Soils. Catena 168, 1–4

Kowalska, J., Mazurek, R., Gasiorek, M., Setlak, M., Zaleski, T., Waroszewski J., 2016. Soil pollution indices conditioned by medieval metallurgical activity - A case study from Krakow (Poland). Environ. Pollut., 218: 1023-1036.

Lizzoli, S., Raigemborn, M.S., Varela, A.N., 2021. Controls of pedogenesis in a fluvial-eolian succession of Cenomanian age in northern Patagonia. Palaeogeography, Palaeoclimatology, Palaeoecology 577, 110549.

Lotfy, H., Abu Heleika, M., Mostafa, R., Wahbah, D., 2017. Africa was still far south in the Late Ypresian: Paleomagnetic study on the early Eocene 'Minia' formation in central Egypt. NRIAG Journal of Astronomy and Geophysics 6, 336–348

Madakka, M. Jayaraju, N. Shirisha J. 2021. An integrated analysis of sinkholes in Kadapa region, Andra Pradesh, India: Implication to Pedology. Microchemical Journal. 170, 106588.

Mange, M. A., Maurer, H. F. W., 1992. Heavy minerals in Colour. Chapman and Hall, London, pp. 147.

Mange, M.A., Wright, D. T., 2007. Heavy Minerals in Use. Developments in Sedimentology, 58, Elsevier, Amsterdam, pp. 1328.

Moghbeli, Z., Owliaie, H., Adhami, E., Najafi-Ghiri, M., Sanjari, S., 2021. Pedogenesis and spatial distribution of soil magnetic properties along a lithotoposequence in an arid region of Southern Iran. Catena 198, 104979.

Moragues-Quiroga, C., Juilleret, J., Gourdol, L., Pelt, E., Perrone, T., Aubert, A., Morvan, G., Chabaux, F., Legout, A., Stille, P., Hissler, C., 2017. Genesis and evolution of regoliths: Evidence from trace and major elements and Sr-Nd-Pb-U isotopes. Catena, 149: 185–198.

Munsell Color, 2009. Munsell Soil-Color Charts with Genuine Munsell Color Chips. 2009 Year Revised/2010 Production. Gretagmacbeth. New Windsor, NY. www.munsell.com

Pansu, M. Gautheyrou, J., 2006. Handbook of Soil Analysis: Mineralogical, Organic and Inorganic Methods. Springer, Berlin, Germany.

Pinheiro Junior, C.R., Pereira, M.G., Azevedo, A.C., Huyssteen, C.V., Anjos, L.H.C., Fontana, A., Neto, E.C.S., Vieira, J.N., Santos, T.G., 2021. Genesis and classification of carbonate soils in the State of Rio de Janeiro, Brazil. Journal of South American Earth Sciences 108, 103183.

Salem, A.A., 2015. Hydrogeological studies on the shallow aquifers in the area west Samalot, El-Minia Governorate, Egypt. Egy. J. Pure & Appl. Sci. 53 (4), 49–60.

Salman, A.K., Aldulaimy, S.E., Mohammed, H.J., Abed, Y.M., 2021. Performance of soil moisture sensors in *gypsiferous* and salt-affected soils. Biosystems engineering 209, 200-209.

Schaetzl, R. J., Anderson, S., 2005. Soils: Genesis and Geomorphology. Cambridge University Press, Cambridge, p. 817.

Schoeneberger, P.J., Wysocki, D.A., Benham, E.C., Soil Survey Staff, 2012. Field book for describing and sampling soils. Version 3.0. Natural Resources Conservation Service, National Soil Survey Center, Lincoln, NE.

Shabana, A.R., 2010. Hydrogeological studies on the Area West Deir Mouas-Mallawi, El-Minia Governorate, Egypt. Egypt. J. Geol. 54, 61–78.

Siqueira, R.G., Schaefer, C.G.R., Filho, E.I.F., Correa, G.R., Francelino, and M.R., Souza, J.J.L., Rocha, P.A., 2021. Weathering and pedogenesis of sediments and basaltic rocks on Vega Island, Antarctic Peninsula. Geoderma 382, 114707.

Soares, M.V., Basilici, G., Lorenzoni, P., Colombera, L., Mountney, N.P., Martinelli, A.G., Mesquita, A.F., da Silva Marinho, T., Garcia, V., Marconato, A., 2020. Landscape and depositional control son paleosols of a distributive fluvial system (Upper Cretaceous, Brazil). Sediment. Geol. 409, 105774.

Soil Science Division Staff, 2017. Soil Survey Manual. United States Department of Agriculture (USDA), Agriculture Handbook No. 18. Natural Resources Conservation Service, Washington, D.C.

Soil Survey Staff, 2014a. Keys to Soil Taxonomy. 12th ed. USDA-Natural Resources Conservation Service, Washington, DC.

Soil Survey Staff, 2014b. Kellogg Soil Survey Laboratory methods manual. Soil Survey Investigations. Report No. 42, version 5.0. R. Burt and Soil Survey Staff (eds.). Washington DC: U.S. Department of Agriculture-Natural Resources Conservation Service.

Su, Y.Z., Zhao, H.L., Zhao, W.Z., Zhang, T.H., 2004. Fractal features of soil particle size distribution and the implication for indicating desertification. Geoderma 122, 43–49.

Sulieman, M.M., Sallam, A.S., Brevik, E.C., Al-farraj, A.S., 2021. Early indicators of pedogenesis at Harrat Khaybar volcano, Saudi Arabia. Geoderma, 383, 114743.

Woodruff, L., Cannon, W. F., Smith, D. B., Solano, F., 2015. The distribution of selected elements and minerals in the soil of the conterminous United States. J. Geochem. Explor., 154: 49-60.

Yang, H. F., Yang, S. L., Xu, K. H., Milliman, J. D., Wang, H., Yang, Z., Chen Z., Zhang, C. Y., 2018. Human impacts on sediment in the Yangtze River: A review and new perspectives. Global and Planetary Change, 162: 8-17.

Yousif, M., Sabet, H.S., Ghoubachi, S.Y., Aziz, A., 2018. Utilizing the geological data and remote sensing applications for investigation of groundwater occurrences, West El Minia, Western Desert of Egypt. NRIAG Journal of Astronomy and Geophysics 7, 318–333

الملخص العربي

أصل وتجانس بعض أراضي غرب المنيا ، الصحراء الغربية ، مصر

عادل عبدالحميد علوان خليل

قسم البيدولوچي، شعبة مصادر المياه والأراضي الصحراوية، مركز بحوث الصحراء، القاهرة، رقم بريدي 11753

أُجريت هذه الدراسة على بعض أراضي غرب إلمنيا بمنطقة درب البهنساوي بالظهير الصحراوي الغربي لمحافظة إلمنيا والتي تغطي حوالي 135 ألف فدان ، بهدف التعرف على أصل تكوينها ومدى تجانس قطاعات التربة بها. تم دراسة عدد 216 قطاع تربة من خلال شبكة منتظمة لتغطية كافة الإختلافات الموجودة بالسهل الرسوبي Alluvial plain بمنطقة الدراسة. تم إختيار وتصميم مقطع عرضي Horizontal toposequence transect بناءاً على طبوغرافية المنطقة Land topograpghy على أساس الإختلاف في الإرتفاعات الأرضية عن منسوب سطح البحر. تم الإنتهاء من الدراسة البيدومورفولوچية التفصيلية في الحقل، وكذلك التحليلات المعملية لبعض صفات التربة الطبيعية والكيميائية التي تخدم الغرض من الدراسة ، كما تم التعرف على الصفات المنرالوجية لعينات التربة الممثلة لآفاق/طبقات القطاعات الارضية المُمَثَّلة عبر اراضي المقطع المختار toposequence transect من خلال تحديد التوزيع الحجمى للحبيبات Particle size distribution، وفصل مكون الرمل الذى تتراوح حجومه ما بين 0.25 – 0.063 مم للتعرف على مكوناته من المعادن الثقيلة والخفيفة Light and heavy minerals بواسطة الفحص الميكروسكوبى. كما تم حساب أدلة التجانس Uniformity indices (UV1, UV2) لقطاعات التربة بُناءً على التوزيع الحجمي للحبيبات للوقوف على درجة تجانسها وإكتشاف Lithologic discontinuities بين طبقاتها، للتعرف على ظروف بيئات الترسيب المختلفة. بالاضافة إلى دراسة العلاقة بين مجاميع المعادن الثقيلة Heavy minerals من خلال حساب نسب التجوية Weathering ratios بين المعادن المقاومة للتجوية Weathering resistant minerals وهى: الزركون والتورمالين والروتيل كمقياس لمدى تجانس مادة الأصل Uniformity ،إعتماداً على بعض هذه المعادن لمعرفة أنوع مواد الأصل المتكونة منها القطاعات الأرضية المدروسة وكذلك للوقوف على مدى نضح الرواسب الأرضية من خلال دليل ZTR. حيث أشارت النتائج إلى أن أغلب القطاعات تكونت من مواد أصل مختلفة بُناءً على دليل UV1 والذي أكده دراسة توزيع محتوى التربة من Coarse fragments رأسياً خلال القطاع الأرضي، وكذلك أكدته الدراسة المنرالوجية. أوصت الدراسة إستخدام دليل UV1 والمُعتمد في حسابه على مكوني الرمل والسلت هو الأكثر مُلائمة لدراسة تجانس التربة مقارنة بـ UV2 والمُعتمد على مكونات التربة الثلاثة (الرمل، السلت، والطين) ويرجع ذلك إلى أن مكوني الرمل والسلت وكذلك Coarse fragments هم أكثر ثباتاً من مكون الطين الذي يتغير بالعمليات البيدوجينية داخل القطاع الأرضي. كما أوضحت الدارسة المعدنية لمكون الرمل (63–250 ميكرون) أن المعادن الخفيفة Light minerals تتميز بسيادة معدن الكوارتز بالمقارنة بمعادن الفلسبارات. وأشارت النتائج إلى زيادة نسبة المعادن الثقيلة Heavy minerals بزيادة الإنحدار وتراوحت ما بين 1,46% في أراضي ذات الإرتفاعات العالية Higher slope soils إلى 16,34% في الأراضي منخفضة الارتفاعات Lower slop soils، حيث إحتوت المعادن الثقيلة على المعادن المعتمة (39,33–61,33%) والمعادن غير المعتمة وهي كالتالي: البيروكسين (الأوجيت والهيبرثين)، الأمفيبول (الهورنبلند والأكتينولايت)،الجارنت،الأستورولايت، الكاينيت، الزيركون، التورمالين، الروتيل، الأبيدوت، الزيوسيت، البيوتيت، المونازيت، الجلاكونايت) بنسب مختلفة حسب الإرتفاع عن منسوب سطح البحر. تم حساب بعض الأدلة (Wr1, Wr2, Wr3, and ZTR) ، إعتماداً على بعض هذه المعادن لمعرفة أنوع مواد الأصل المتكونة منها القطاعات الأرضية المدروسة وكذلك للوقوف على مدى نضح الرواسب الأرضية عبر المتسلسلة الأرضية لكل وادي. كما أكدت الدراسة المنرالوجية أماكن Lithologic discontinuities التي تم إكتشافها بالصفات البيدومورفولوجية والطبيعية ما بين طبقات القطاع الأرضي مؤكدة عدم تجانس مواد الأصل التي تكونت منه الرواسب الأرضية. وفي ضوء ما توصلت إليه الدراسة فقد نوقشت النتائج في محاوله للتمييز بين أنواع الأراضي تحت الدراسة بناءً على درجة تطورها ونضجها. خُلصت نتائج الدراسة إلى أن الأراضي تحت الدراسة حديثة النشأة والتكوين، كما تواجد نوعان أساسيان من عمليات تكوين التربة من أجل تطور آفاق كالسية وأخرى

جبسية عبر المقطع الطبوغرافي المدروس، كما أظهرت منحنيات التوزيع الرأسي للمعادن الأكثر مقاومة للتجوية رأسيا داخل القطاعات المدروسة نمطاً غير منتظماً مما أثيت عدم تجانس مادة أصل التربة وتكوينها تحت بيئات ترسيب متعاقبة بصورة مختلفة وقد دعمت أدلة التجانس والمستخدمة في البحث هذه النتائج. كما تم دراسة مراحل تطور الأراضي المتأثرة بالجبس عبر أراضي المقطع الطبوغرافي.